



HAL
open science

A loss-of-function mutation in AtYSL1 reveals its role in iron and nicotiananmine seed loading.

M. Lejean, A. Schikora, S. Mari, J.F. Briat, Catherine Curie

► To cite this version:

M. Lejean, A. Schikora, S. Mari, J.F. Briat, Catherine Curie. A loss-of-function mutation in AtYSL1 reveals its role in iron and nicotiananmine seed loading.. *Plant Journal*, 2005, 44 (5), pp.769-782. 10.1111/j.1365-313X.2005.02569.x . hal-00086381

HAL Id: hal-00086381

<https://hal.science/hal-00086381>

Submitted on 20 Dec 2020

HAL is a multi-disciplinary open access archive for the deposit and dissemination of scientific research documents, whether they are published or not. The documents may come from teaching and research institutions in France or abroad, or from public or private research centers.

L'archive ouverte pluridisciplinaire **HAL**, est destinée au dépôt et à la diffusion de documents scientifiques de niveau recherche, publiés ou non, émanant des établissements d'enseignement et de recherche français ou étrangers, des laboratoires publics ou privés.

A loss-of-function mutation in *AtYSL1* reveals its role in iron and nicotianamine seed loading

Marie Le Jean, Adam Schikora, Stéphane Mari, Jean-François Briat and Catherine Curie*

Biochimie et Physiologie Moléculaire des Plantes, CNRS (UMR 5004)/INRA/Agro-M/Université Montpellier II, 2 place Viala, F-34060 Montpellier Cedex 1, France

Received 18 April 2005; revised 26 August 2005; accepted 30 August 2005.

*For correspondence (fax +33 467 52 5737; e-mail curie@ensam.inra.fr).

Summary

The Arabidopsis Yellow Stripe 1-Like (YSL) proteins have been identified by homology with the maize (*Zea mays*) Yellow Stripe 1 (YS1) transporter which is responsible for iron–phytosiderophore (PS) uptake by roots in response to iron shortage. Although dicotyledonous plants do not synthesize PS, they do synthesize the PS precursor nicotianamine, a strong metal chelator essential for maintenance of iron homeostasis and copper translocation. Furthermore, ZmYS1 and the rice (*Oryza sativa*) protein OsYSL2 have metal-nicotianamine transport activities in heterologous expression systems. In this work, we have characterized the function of *AtYSL1 in planta*. Two insertional loss-of-function *ysl1* mutants of Arabidopsis were found to exhibit increased nicotianamine accumulation in shoots. More importantly, seeds of both *ysl1* knockouts contained less iron and nicotianamine than wild-type seeds, even when produced by plants grown in the presence of an excess of iron. This phenotype could be reverted by expressing the wild-type *AtYSL1* gene in *ysl1* plants. *ysl1* seeds germinated slowly, but this defect was rescued by an iron supply. *AtYSL1* was expressed in the xylem parenchyma of leaves, where it was upregulated in response to iron excess, as well as in pollen and in young silique parts. This pattern is consistent with long-distance circulation of iron and nicotianamine and their delivery to the seed. Taken together, our work provides strong physiological evidence that iron and nicotianamine levels in seeds rely in part on *AtYSL1* function.

Keywords: YSL, iron, nicotianamine, transport, seed, circulation.

Introduction

Iron (Fe) is an essential element for living organisms, and plants play a major role in its entry into the food chain. Because Fe bioavailability is often low in soils, plants have evolved efficient uptake strategies that can be classified into two types (Curie and Briat, 2003; Römheld and Marschner, 1986). Non-grass plants have adopted the so-called strategy I, in which Fe(II) transport is coupled to a Fe(III)-chelate reduction step. This strategy is sensitive to alkaline pH and is therefore less efficient in calcareous soils, which represent up to 30% of arable land world-wide. Molecular components of this uptake strategy have been characterized in Arabidopsis. The plasmalemma root ferric-chelate reductase FRO2 reduces soil Fe(III) (Robinson *et al.*, 1999) and provides Fe(II) for IRT1, a major metal transporter that takes up Fe(II) into the root epidermis (Eide *et al.*, 1996; Henriques *et al.*, 2002; Varotto *et al.*, 2002; Vert *et al.*, 2002). The FRO2 and IRT1 genes are co-regulated in response to plant Fe status at both the transcriptional and

the post-transcriptional levels, through complex pathways integrating signals such as local Fe concentration and uncharacterized long-distance signaling molecules (Connolly *et al.*, 2002, 2003; Eide *et al.*, 1996; Robinson *et al.*, 1999; Vert *et al.*, 2003). Grasses, or strategy II plants, such as maize (*Zea mays*), are less susceptible to chlorosis on calcareous soils because their uptake mechanism relies on the efficient chelation/solubilization of Fe(III). In response to Fe deficiency, grasses synthesize non-proteinogenic amino acids of the mugineic acid family, derived from S-adenosyl methionine and commonly called phytosiderophores (PS; Takagi *et al.*, 1984). PS are secreted in the rhizosphere where they chelate various metals, including Fe(III), with a very strong affinity. Fe(III)–PS complexes are then taken up into the root by a specific transporter encoded by the Yellow Stripe 1 (YS1) gene in maize (Curie *et al.*, 2001; von Wiren *et al.*, 1994). Expression of ZmYS1 in heterologous systems has shown that YS1 functions as

a proton-coupled symporter for phytosiderophore-chelated metals (Curie *et al.*, 2001; Roberts *et al.*, 2004; Schaaf *et al.*, 2004).

Distribution of Fe to the various plant organs involves its long-distance transport through the sap. In the xylem, Fe is thought to be mainly chelated to organic acids such as citric or malic acid. In the phloem, which supplies micronutrients to roots and developing organs, the transport of Fe causes problems because of the high pH (between seven and eight) of this compartment and the propensity of Fe ions to precipitate in alkaline solution. In *Ricinus communis* seedlings, a binding partner of Fe(III) has been identified as a small protein of the late embryogenesis abundant (LEA) family, called the iron transport protein (ITP; Krüger *et al.*, 2002). Nicotianamine (NA), a strong chelator of transition metals (von Wiren *et al.*, 1999), is likely to chelate Fe(II) in the phloem as Fe(II)–NA is very stable at pH 7 or above and as NA is abundant in phloem sap. NA is a precursor and a structural analog of PS, which is present in both strategy I and strategy II plants. The role of NA in Fe homeostasis is illustrated by the numerous Fe metabolism defects presented by the tomato (*Lycopersicon esculentum*) NA-less mutant *chloronerva*, which is chlorotic despite the presence of a high concentration of Fe in its leaves and constitutive activity of its root Fe uptake system, and which fails to flower if not supplied with exogenous NA (Higuchi *et al.*, 1996; Ling *et al.*, 1999; Stephan *et al.*, 1996). In addition, a tobacco plant (*Nicotiana tabacum*) deficient in NA was engineered via overproduction of the barley (*Hordeum vulgare*) nicotianamine amino transferase (NAAT) enzyme which consumes NA (Takahashi *et al.*, 2003). This *naat* plant presents pleiotropic phenotypes, including interveinal chlorosis of young leaves, abnormally shaped and mostly sterile flowers, and rare and incompletely developed seeds, all of these defects being related to a shortage in transition metal and more specifically Fe delivery to plant organs.

Schaaf *et al.* (2004) have shown that, in addition to metal–PS chelates, maize YS1 can transport metals chelated to NA in heterologous expression systems. As eight YS1-like (YSL) gene sequences sharing a high level of homology with *ZmYS1* were found in Arabidopsis (Curie *et al.*, 2001), we postulated that YSL proteins may transport metal–NA chelates in strategy I plants.

Several laboratories have recently reported work on Arabidopsis and rice YSL2 (DiDonato *et al.*, 2004; Koike *et al.*, 2004; Schaaf *et al.*, 2005). In Arabidopsis, DiDonato *et al.* (2004) showed that expression of *AtYSL2* is able to restore growth of the *fet3fet4* Fe uptake-defective yeast mutant, specifically when Fe is provided as Fe(II)–NA but not as Fe(III)–NA. These authors therefore concluded that *AtYSL2* is a Fe(II)–NA transporter *in planta*. We have obtained contradictory results, as we did not observe any Fe–NA-dependent complementation of the *fet3fet4* mutant by *AtYSL2*, and furthermore established that DiDonato *et al.*'s

growth restoration was independent of Fe or NA supply (Schaaf *et al.*, 2005). *AtYSL2* also failed to mediate Fe(II)–NA-inducible currents in *Xenopus laevis* oocytes (Schaaf *et al.*, 2005). These two reports reached the same conclusions regarding the expression of *AtYSL2* in the vasculature, at the level of xylem-associated cells in roots, and also regarding *AtYSL2* downregulation in response to Fe deficiency. We have additionally observed that *AtYSL2* expression strongly decreases upon zinc starvation (Schaaf *et al.*, 2005). In transgenic plants expressing the *AtYSL2::GFP* fusion protein, fluorescence was observed on the lateral sides of the xylem parenchyma plasma membrane (DiDonato *et al.*, 2004). This prompted the authors to propose a role for *AtYSL2* in the lateral movement of metals from the vasculature. In rice, expression of *OsYSL2*, one of 18 putative *OsYSL* genes in this species, is upregulated by Fe deficiency in the leaf, where it is particularly strong in the phloem, and is also observed in developing seeds (Koike *et al.*, 2004). Based on *OsYSL2* localization in the plasma membrane and on electrophysiological experiments in *X. laevis* oocytes, the authors have proposed that *OsYSL2* may be required for long-distance transport of Fe(II)–NA and Mn(II)–NA through the phloem and for their loading into the grain.

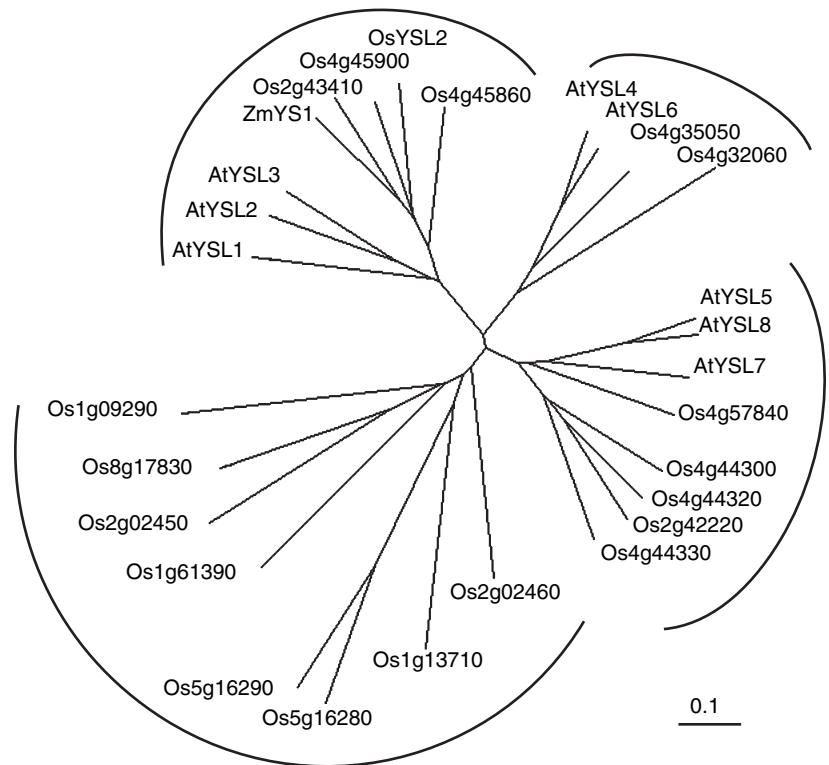
In this study, we show that a functional *AtYSL1* gene is required to produce seeds containing wild-type levels of Fe and NA, and suggest that *AtYSL1* could contribute to the long-distance transport of these compounds via the xylem. *AtYSL1* was expressed in the xylem parenchyma of the leaf, as well as in various parts of the developing flower and silique. *AtYSL1* expression increased in response to an Fe excess. Knocking out *AtYSL1* resulted in disturbances in the levels of NA in leaves and seeds, a decrease in the amount of Fe in seeds, and a slow germination rate. An increased Fe supply rescued germination but did not restore wild-type levels of Fe or NA in mutant seeds, which strongly suggests that at least part of Fe feeding into seeds requires the simultaneous mobilization of NA.

Results

Phylogeny and structural organization of AtYSL1

The Arabidopsis genome contains eight YSL gene sequences encoding putative transmembrane proteins with high homology to *ZmYS1*, the maize founding member of the family (Curie *et al.*, 2001). Eighteen YSL genes have also been reported in rice, and we found a nineteenth member of the family (*Os1g61390*) in the databases (Figure 1). *AtYSL1*, *AtYSL2* and *AtYSL3* are most similar to *ZmYS1* (around 60% similarity) and together form a subfamily among the YSL proteins that includes *OsYSL2* as well as three other rice homologs (DiDonato *et al.*, 2004; Koike *et al.*, 2004; Schaaf *et al.*, 2005) (Figure 1). The YSL proteins are related to the oligopeptide transporter (OPT) family (Yen *et al.*, 2001), but

Figure 1. Phylogenetic tree of proteins of the YSL family from *Arabidopsis thaliana* (AtYSL1-8), *Zea mays* (ZmYS1) and *Oryza sativa* (OsYSL2 and Os accession numbers) generated using the phylogenetic tree printer PhyloDendron (<http://iubio.bio.indiana.edu/treeapp/treeprint-form.html>).



quite distantly as they only share an average of 10% similarity and do not contain the OPT consensus domain (Koh *et al.*, 2002). The open reading frame of *AtYSL1* was amplified from reverse-transcribed *Arabidopsis* total RNA and cloned into a pBluescript vector. It encodes a 673 amino acid-long protein containing 12–14 predicted transmembrane domains and presenting an N-terminal domain predicted to be cytoplasmic (<http://psort.nibb.ac.jp>).

AtYSL1 expression depends on Fe status

The hypothesis that the YSL proteins are involved in metal mobilization prompted us to analyze the pattern of expression of the *AtYSL1* gene in response to metal content variations, with the hope of obtaining an indication on the physiological role of *AtYSL1*. Five-week-old hydroponically grown *Arabidopsis* plants were transferred to medium lacking or not lacking one of the metal ions Fe, manganese (Mn), zinc (Zn) or copper (Cu) and grown for three additional days. Total RNA extracted from these plants was blotted and hybridized with an *AtYSL1*-specific probe (see Experimental procedures). Compared with control conditions, we observed no change in the amount of *AtYSL1* mRNA in Mn, Zn or Cu deficiency (data not shown). Upon Fe-deficiency treatment, however, accumulation of *AtYSL1* transcripts was slightly but significantly reduced (data not shown). This prompted us to test whether *AtYSL1* expression is inducible by an Fe overload. Six-week-old plants were therefore treated with 500 μM Fe following a 5-day period of Fe starvation

to promote the Fe overload response (Lobreaux *et al.*, 1992). The kinetic of accumulation of *AtYSL1* mRNA was assayed by Northern blot in roots and shoots separately [Figure 2(a,b)]. Expression of the ferritin-encoding gene *AtFER1*, which is specifically induced by an Fe excess, was used as a control for the Fe treatment. *AtFER1* mRNA accumulation was detected 6 h after transfer to Fe excess conditions in both roots and shoots and decreased within 12–24 h of treatment. *AtYSL1* mRNA was only detected in shoots where, although detectable in control growth conditions (0 h), its amount increased from 6 h to reach a maximum at 12 h post-treatment, like *AtFER1*. However, unlike *AtFER1*, expression of which decreased after 12 h in shoots, *AtYSL1* gene expression stayed on over the next 3 days of treatment [Figure 2(b)]. Moreover, the induction factor calculated for *AtYSL1* was 10 times smaller (2.5-fold) than that for *AtFER1* (25-fold). We concluded that the *AtYSL1* gene is specifically expressed in shoots and rapidly although moderately induced by Fe excess. Although Cu is a likely ligand for NA, and accumulates in roots of *chloronerva*, we observed no change in *AtYSL1* gene expression in response to Cu deficiency or excess (data not shown).

In order to quantify the *AtYSL1* promoter response to Fe excess, we generated transgenic *Arabidopsis* plants expressing the *uidA* gene, encoding β -Glucuronidase (GUS) gene under the control of 1.5 kb of *AtYSL1* sequences located upstream of the ATG. GUS activity was monitored in shoots of 12 independent transgenic lines selected on kanamycin *in vitro* for 10 days, and then transferred for 5 days onto

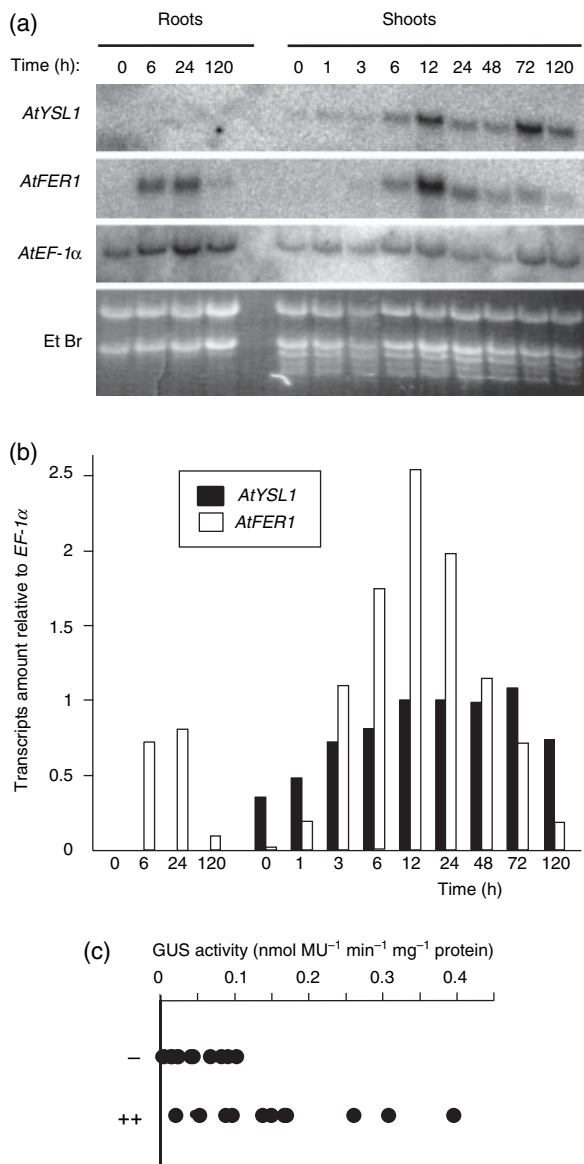


Figure 2. *AtYSL1* gene expression in response to iron nutrition. (a) RNA gel blot showing the kinetics of accumulation of *AtYSL1* mRNA in plant shoots in response to excess iron. Fifteen micrograms of total RNA extracted from 6-week-old plants treated with an excess of 500 μM iron-ethylenediaminetetraacetic acid (Fe-EDTA) for the indicated length of time was blotted and hybridized successively to *AtYSL1*, *AtFER1* and *AtEF-1 α* specific probes. Ethidium bromide (EtBr) staining is shown. (b) Quantification of the RNA gel blot shown in (a) using Image J (<http://rsb.info.nih.gov/ij/>). *AtYSL1* and *AtFER1* transcripts were normalized by the *AtEF-1 α* signal. (c) Enzymatic GUS assay for 12 independent transgenic lines expressing an *AtYSL1* promoter-GUS fusion and grown in the absence of added iron (-Fe) or in the presence of 300 μM of added Fe-EDTA. No significant activity was detected in wild-type plant extracts (data not shown). MU, methylumbelliferone.

media either lacking Fe (-) or supplemented with 300 μM Fe (++). The mean of the enzymatic GUS activities, assayed by fluorometry, was around 0.04 nmol MU $^{-1}$ min mg $^{-1}$ protein

in control conditions, while it reached 0.16 nmol MU $^{-1}$ min mg $^{-1}$ protein in high Fe conditions, indicating a 4-fold induction of *AtYSL1* promoter activity in response to Fe excess [Figure 2(c)]. This result is consistent with the 2.5-fold induction of *AtYSL1* mRNA accumulation measured by Northern blotting.

Tissue-specific expression of *AtYSL1*

To gain insight into the biological function of *AtYSL1*, we looked at the tissues and cell types expressing *AtYSL1*. Histochemical analyses were performed using the above-mentioned Arabidopsis transgenic lines expressing an *AtYSL1* promoter-GUS fusion. Plants were grown *in vitro* for 2 weeks in the presence of various amounts of Fe as indicated in the legend to Figure 3. Staining of entire plantlets confirmed that the *AtYSL1* promoter was active in shoots but not in roots (data not shown). In leaves, GUS activity was restricted to the veins and, although visible in the absence of Fe in the medium [Figure 3(a)], it increased with Fe concentration, spreading to neighboring mesophyll cells at 300 μM Fe [Figure 3(b,c)]. A cross-section of the basal part of a leaf treated as in Figure 3(b) showed that the staining was restricted to the xylem pole of primary and secondary veins and more specifically to the xylem parenchyma surrounding xylem tubes [Figure 3(d,e)]. In flowers, we observed GUS activity in the vasculature of sepals and petals as well as in pollen grains [Figure 3(f-h)]. A faint staining was generally visible on the style, underneath the stigmatic papillae [Figure 3(g)]. Staining of pollen grains was observed in young flowers, when anthers are still positioned well below the stigma, and disappeared at stages with fully elongated anthers [Figure 3(f)]. Counter-staining of blue pollen grains with 4, 6-diamidino-2-phenylindole (DAPI) showed the presence of three nuclei, one vegetative and two generative, indicating that pollen grains expressing GUS have already reached the mature stage [inset of Figure 3(h)]. In senescing stamens, coloration of the anthers disappeared whereas strong GUS staining was seen in the vascular tissue of the filament [Figure 3(i)].

The *AtYSL1* promoter is also active in siliques (Figure 4). We observed strong staining in the petiole next to the abscission zones of the sepals, petals and stamens where it increased upon maturation of the silique [Figure 4(a)]. A close-up view of the abscission region revealed coloration of the vessels connected to each flower whorl [Figure 4(c)]. A cross-section of the petiole indicated that the GUS activity was restricted to the xylem parenchyma [Figure 4(f)]. In addition to the petiole, staining was observed in very young siliques at the level of the carpel veins, in the style underneath the stigmatic papillae [Figure 4(e)] and in a small region of the developing seed [Figure 4(d)]. Only the staining in the style persisted in mature siliques [Figure 4(a)]. A cross-section of a very young silique containing seeds at a very early stage of

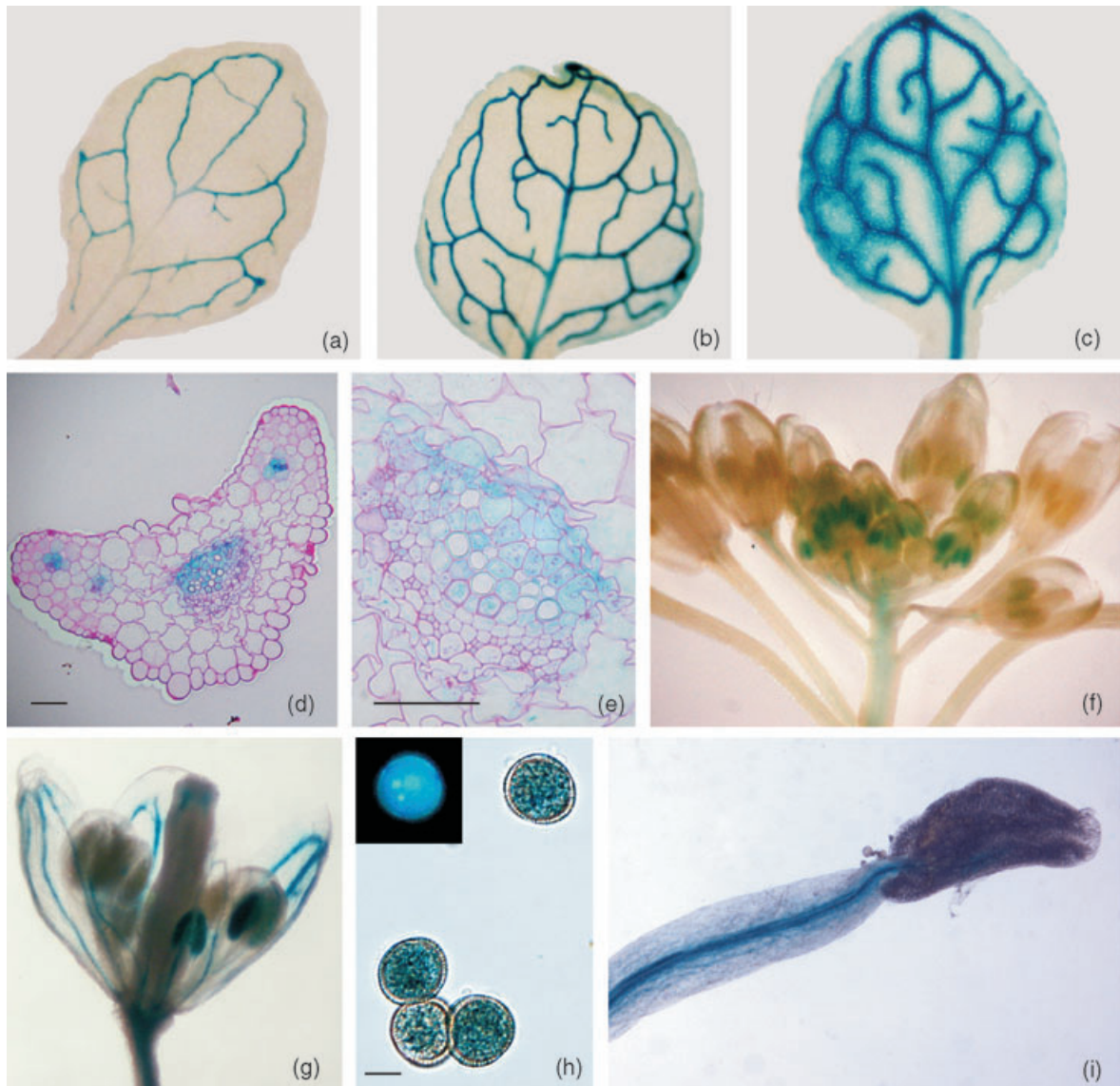


Figure 3. Cell type-specific localization of *AtYSL1* gene expression.

(a–e) GUS histochemical staining of leaves of 15-day-old transgenic plantlets grown on various iron-ethylenediaminetetraacetic acid (Fe-EDTA) concentrations: (a) no added Fe; (b, d, e) 50 μM Fe; (c) 300 μM Fe.

(d, e) Cross-section through the base of a leaf; (e) higher magnification of the midvein; (f) the inflorescence; (g) the immature flower; (h) pollen grains, with inset of 4, 6-diamidino-2-phenylindole (DAPI) staining showing one large vegetative nucleus and two small dense generative nuclei; (i) the senescing stamen. ep, epidermis; mv, midvein; p, parenchyma; st, stomata; sv, secondary vein. Bar, 10 μm in (h) and 200 μm in (d) and (e).

development showed GUS activity in cells surrounding xylem tubes in the silique envelope [Figure 4(g)]. In addition, inside the locule, GUS activity was detected in the vascular tissue of the funiculus and at the basis of the funiculus in the posterior pole of the ovule, a region corresponding to the chalazal endosperm [Figure 4(g)].

Characterization of an Arabidopsis ysl1-1 knockout plant

We and others have previously shown that expression of the first member of the YS gene family, the maize *YS1*

gene, can functionally complement the yeast Fe uptake defect when Fe is provided as an Fe-PS chelate (Curie *et al.*, 2001; Schaaf *et al.*, 2004). However, we did not succeed in showing such heterologous complementation with *Arabidopsis YSL2* (Schaaf *et al.*, 2005). We also failed to show growth restoration mediated by *AtYSL1* expression on media containing Fe(II)-NA, Fe(III)-NA or Fe(III)-PS (data not shown). We therefore addressed the biological function of *AtYSL1* *in planta* by scrutinizing the physiological alterations resulting from knocking out the *AtYSL1* gene.

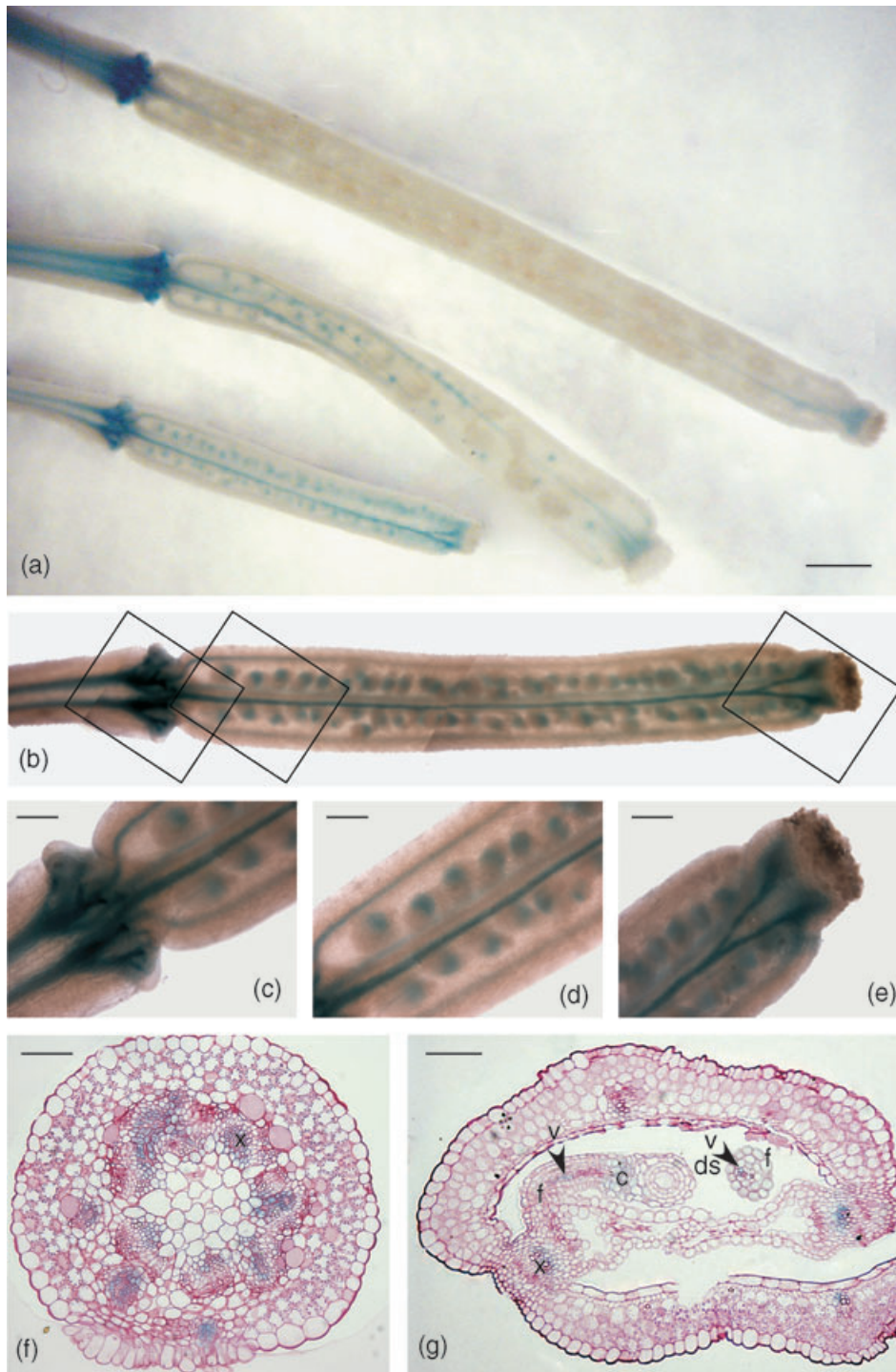
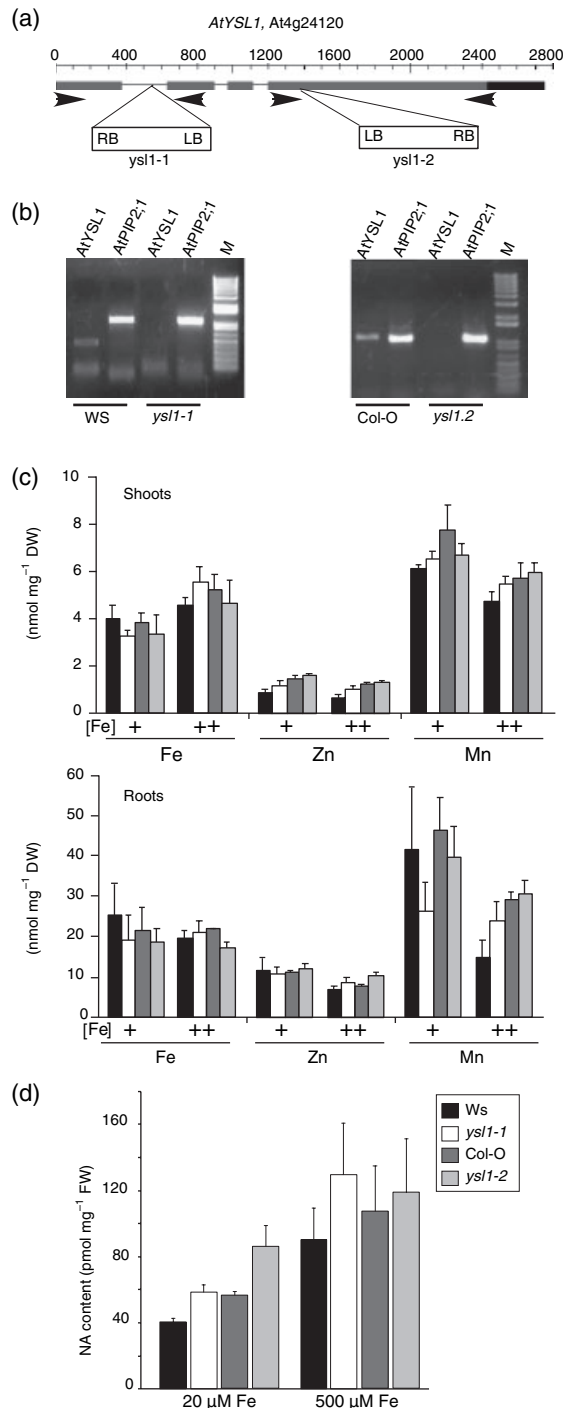


Figure 4. *AtYSL1* gene expression in siliques. GUS histochemical staining of siliques removed from soil-grown plants is shown. (a) Binocular observation of siliques at different developmental stages. (b–e) Early-stage siliques observed using an optical microscope. (b) The entire silique reconstituted from several images obtained with an optical microscope. (c, d, e) Boxed regions are shown at higher magnification (c, petiole; d, central part; e, style and stigmat). (f) A 5- μ m cross-section of a silique petiole near the abscission zone. (g) A 5- μ m cross-section of the young silique shown in (b). f, funiculus; ds, developing seed; c, chalaza; v, vein; x, xylem. Bar, 500 μ m (a), 100 μ m (c, d, e) or 50 μ m (f, g).

The release of flanking sequence tags (FST) for Arabidopsis T-DNA insertion lines from the Versailles-Institut National de la Recherche Agronomique (INRA) laboratory (Versailles, France) and from the SIGnAL program (Salk Institute, La Jolla, CA, USA) identified two insertion lines in the *AtYSL1* gene. Line DRM20 in the ecotype Wassilewskija (Ws), named *ysl1-1*, and line SALK_034534 in the ecotype Columbia (Col-0), named *ysl1-2*, contain a single T-DNA inserted respectively



in the first intron and in the fourth exon of the gene in the orientation indicated in Figure 5(a). Using PCR on reverse-transcribed mRNA prepared from the *ysl1-1* and *ysl1-2* lines, we amplified an *AtYSL1*-specific fragment with wild-type Ws or Col-0 samples but none with *ysl1-1* or *ysl1-2* samples, whereas the control aquaporin *AtPIP2;1* gene-specific band was obtained with both wild-type and mutant plants [Figure 5(b)]. The absence of *AtYSL1* transcripts thus confirmed that *ysl1-1* and *ysl1-2* are null alleles of *AtYSL1*.

ysl1 homozygous mutants did not show any change in macroscopic phenotype, either on soil or *in vitro*. Moreover, variation of the metal content, i.e. an excess or deficiency of Fe, Cu, Mn or Zn, did not reveal any growth defect (data not shown). We then measured the metal content in the two mutant lines and in their parental wild-type background. Five-week-old hydroponically grown plants were transferred, after a 5-day period of Fe starvation, to either low Fe-containing medium (20 μM) or excess Fe (500 μM) for 3 days. Measurement of metal ions was performed using an atomic absorption spectrometer (AAS) on shoots and roots harvested separately. We found no significant variation in Fe, Zn or Mn content between wild-type and mutant plants, either in shoots or in roots [Figure 5(c)].

If the physiological role of *AtYSL1* is to transport NA-metal complexes into or out of the xylem, one might expect to see a modification of NA distribution between shoots and roots. NA was detected by high-performance liquid chromatography (HPLC) analysis on shoots of the tissue samples previously subjected to AAS analysis. Upon treatment with 20 μM Fe, shoots of both *ysl1* mutants were found to contain around 40% more NA than their respective wild type [Figure 5(d)]. At high Fe concentration, we observed an increase of NA content in the mutant, the extent of which was difficult to evaluate because of elevated standard errors, although this increase was smaller than that in low Fe [Figure 5(d)]. We concluded that *AtYSL1* moderately but significantly contributes, directly or indirectly, to NA content in leaves.

Figure 5. Characterization of two *AtYSL1* gene knockout lines.

(a) Schematic representation of the T-DNA integration site in the *AtYSL1* genomic sequence for *ysl1-1* and *ysl1-2* mutant lines. Exons are represented by boxes and introns by lines. Orientation of the T-DNA copies is shown. (b) Absence of *AtYSL1* transcript in *ysl1-1* and *ysl1-2* plants. An ethidium bromide-stained DNA gel is presented showing reverse transcriptase-polymerase chain reaction (RT-PCR) amplification fragments corresponding to *AtYSL1* or Arabidopsis Plasma membrane Aquaporin 2;1 (*AtPIP2;1*) (control) transcripts in wild-type and mutant alleles. Arrowheads indicate the position of *AtYSL1* primers. (c) Iron (Fe), zinc (Zn) and manganese (Mn) content determined by atomic absorption spectrometer (AAS) in shoots or roots of wild-type and mutant alleles of *AtYSL1* grown as above. (d) Nicotianamine content measured by high-performance liquid chromatography (HPLC) in shoots of wild-type and mutant plants. Plants were grown for 5 weeks in hydropony, washed, transferred for 5 days to Fe-less medium and then transferred again for 3 days to either low iron-containing medium (20 μM, +) or high iron-containing medium (500 μM, ++). Values are the mean of three samples (c, d).

Knocking out the *AtYSL1* gene resulted in decreased Fe and NA content in seeds

The fact that GUS expression is in part localized in the young silique, both in the vascular tissue and at the level of the chalazal end of the seed, suggests that *AtYSL1* could be involved in Fe loading via Fe–NA transport into the seed. We therefore asked whether NA content is modified in the seeds of the *ysl1* mutants. Using HPLC analysis, we found an almost 2-fold decrease in the amount of NA in *ysl1-1* and a 4-fold decrease in *ysl1-2* [Figure 6(a)]. We previously showed that addition of FeEDDHA to the growth solution can fully rescue the severe Fe deficiency of an *IRT1*-less mutant in *Arabidopsis* (Vert *et al.*, 2002). However, this defect in NA accumulation was not rescued when seeds were harvested from *ysl1-1* plants watered with 0.6 mM FeEDDHA [Figure 6(b)]. Furthermore, compared with the wild type, the Fe content of *ysl1* seeds was altered for both mutant alleles, although to a different extent: *ysl1-1* seeds contain 65% less iron than *Ws* seeds whereas *ysl1-2* seeds contain 30% less iron than *Col-0* seeds [Figure 6(c)]. FeEDDHA watering of plants barely increased the Fe content in wild-type seeds (by <20%), and did not rescue Fe deficit in *ysl1-1* seeds [Figure 6(d)]. Therefore, exogenous addition of Fe during plant growth did not correct deficiencies in the NA or Fe content of *ysl1* seeds. Finally, the metal concentration in seeds of both *ysl1* alleles, determined by inductively coupled plasma mass spectrometry (ICP-MS), revealed no variations in Cu and Zn content, but a significant accumulation of Mn [Figure 6(e)], which could result from the deregulation of another metal transporter in response to the change of seed Fe status.

To further confirm that a defective *AtYSL1* gene was responsible for the physiological disorders observed in *ysl1-1* and *ysl1-2* seeds, we investigated whether expressing the wild-type *AtYSL1* gene in *ysl1-1* could rescue its phenotype. Eight such transgenic *ysl1-1:AtYSL1* plants were generated and their Fe and NA contents were determined in seeds (Figure 7). We found the levels of Fe and NA in the different complemented lines to spread roughly between the values measured in knockout and wild-type seeds. This heterogeneity is consistent with the position effect observed in independent transgenic lines and probably explains why one complemented mutant had a NA concentration in seeds that was up to 30% higher than that of the wild type [Figure 7(b)]. Thus, expression of a wild-type *AtYSL1* gene in a *ysl1* knockout can efficiently rescue disorders in its seed physiology.

ysl1.1 germination is slower on Fe-deficient medium

Finally, given that seeds of *ysl1-1* knockout plants are Fe-deficient, we looked for a defect in seed germination on media containing a range of Fe concentrations. Seeds of *Ws* and *ysl1-1*, produced by water- or FeEDDHA-irrigated plants,

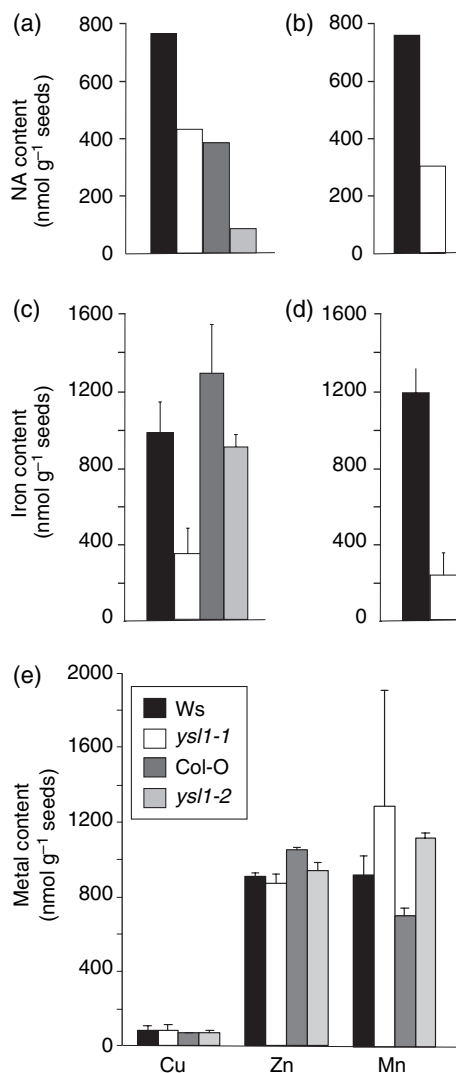


Figure 6. Disorders of seed physiology in *ysl1* mutants. (a, b) Nicotianamine content in *ysl1* and wild-type seeds set by plants irrigated with water (a) or with 600 μM FeEDDHA (b). (c, d) Iron content in seeds obtained as in (a) and (b), respectively. (e) Metal content in seeds of wild-type and mutant plants measured by inductively coupled plasma mass spectrometry (ICP-MS). Values are the mean of three samples (c–e).

were sown on agar plates supplemented with 0, 50 or 350 μM Fe. The number of germinated seeds, i.e. seeds with an emerging radicle, counted once a day from 48 to 120 h post-sowing is represented as a percentage of the total number of seeds [Figure 8(a,b)]. On Fe-deficient plates, <40% of the *ysl1-1* seeds had germinated at 48 h compared with >65% of the *Ws* seeds [Figure 8(a)]. This difference decreased over time and had almost vanished at 96 h after sowing. Seeds from FeEDDHA-watered plants showed the same curve of germination [Figure 8(a)]. In the presence of a high concentration of Fe in the plate, however, mutant and wild-type

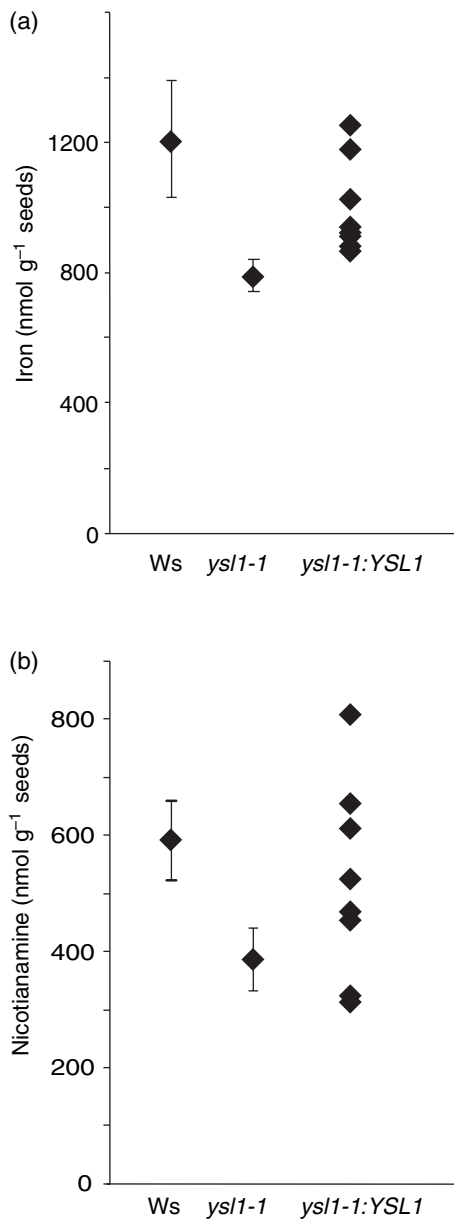


Figure 7. Expression of *AtYSL1* in *ysl1-1* mutant restores its seed physiological disorders.

(a) Seed nicotianamine content.

(b) Seed iron content. Values are the mean of three measurements.

seeds did not show a significant difference [Figure 8(b)]. An intermediate response of the mutant was obtained at 50 μM Fe, as 45% of the mutant seeds had germinated at 48 h and the percentage germination had already caught up with that of the wild type at 72 h (data not shown).

On Fe-starved plates, compared with *Ws*, *ysl1-1* plants exhibited a shorter radicle, bleached cotyledons and a lack of anthocyanin-characteristic pink stain [Figure 8(c), panels (a) and (b)]. On plates containing high Fe, however, the wild type and mutant were undistinguishable [Figure 8(c), panels

(c) and (d)]. We concluded that mutation in *AtYSL1* results in a transient defect of germination, which can be rescued by Fe supply during germination, but not by the accumulation of Fe during the vegetative life of the plant.

Discussion

In this work, we have established that the *AtYSL1* transporter is necessary for correct loading of Fe and NA into Arabidopsis seeds, as seeds of two independent knockout plants lacking a functional *AtYSL1* gene were found to have reduced levels of NA and Fe, and as normal levels could be restored by expression of a wild-type *AtYSL1* gene. This strongly suggests that *AtYSL1* participates in Fe loading of the seed via its transport as an Fe–NA chelate. Such a function is supported by the strong expression of *AtYSL1* in tissues surrounding xylem vessels in the silique as well as in the chalazal endosperm of the seed, a region that adjoins the maternal vascular tissue to the seed integuments and which could be involved in the transfer of nutrients to the embryo (Nguyen *et al.*, 2000) and in mineral storage (Otegui *et al.*, 2002). Direct evidence of the transport activity and substrate of *AtYSL1* is still lacking, in contrast to the situation for two other YSL family members, *ZmYS1* and *OsYSL2*, which have been shown to transport Fe–NA chelates in heterologous expression systems (Koike *et al.*, 2004; Schaaf *et al.*, 2004). Nevertheless, based on reverse genetics, our study provides *in planta* evidence of the involvement of YSL transporters in NA allocation in a specific plant organ. We found the ratio between Fe decrease and NA decrease to vary between the two mutant alleles and between two experiments with one allele (Figures 6 and 7). Such fluctuations may be explained by the fact that the concentrations of metabolites and nutrients are modulated by environmental cues and according to the physiological state of the plant. However, in all our experiments, NA and Fe concentrations in seeds showed the same tendency to decrease in both *ysl1* mutants, while this tendency was either reduced or inverted in the complemented mutant lines.

The fact that growth of plants in the presence of 600 μM FeEDDHA did not allow recovery of normal Fe levels in the *ysl1-1* mutant seeds supports the hypothesis that Fe loading in the seed requires that Fe is provided as a specific chelate. This is consistent with earlier data showing that the pea (*Peasum sativum*) E107 mutant, which contains 36 times more Fe in its leaves than wild-type Sparkle pea, does not translocate more Fe in seeds than the wild type, suggesting that a specific chelate must be loaded in the phloem to feed the seed (Grusak, 1994). The possibility exists that *AtYSL1* could transport a chelate other than Fe–NA. As the Arabidopsis NA synthase-encoding genes are differentially regulated by Fe nutrition (N. K. Nishizawa, Laboratory of Plant Biology, University of Tokyo, Tokyo, Japan, personal communication), the decrease in seed NA content could in fact

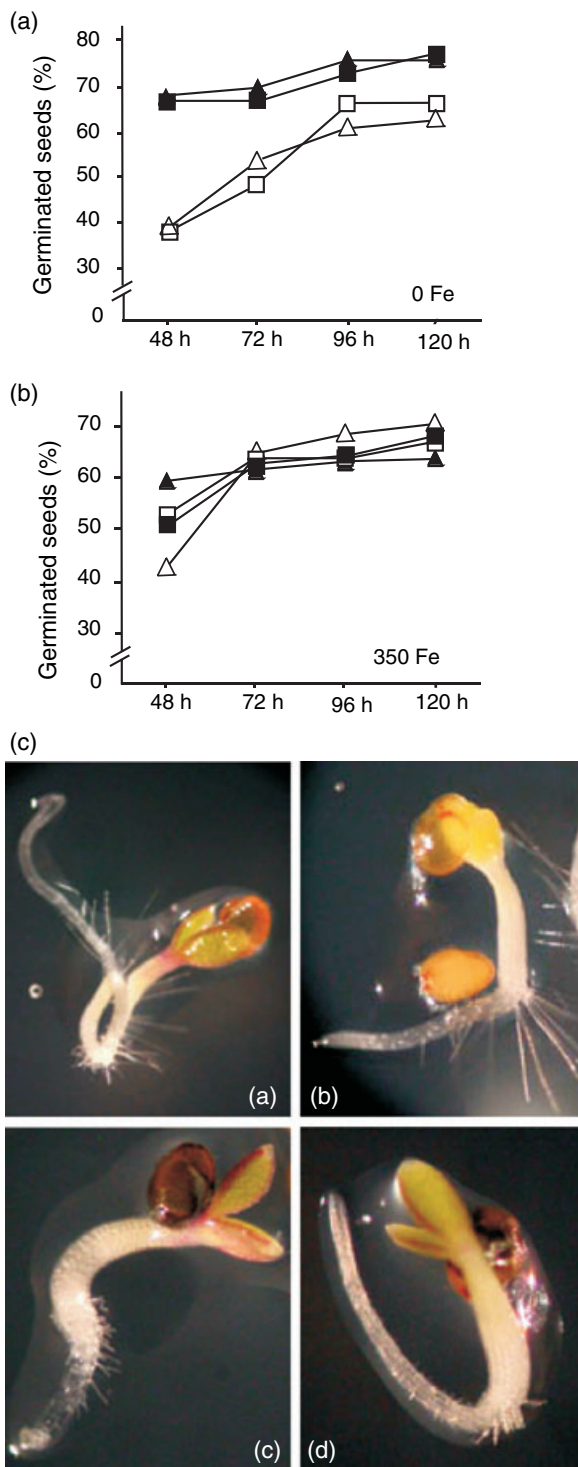


Figure 8. Germination defect of *ysl1-1* mutant seeds. (a, b) Germination rate between 48 and 120 h after sowing on iron-deprived medium (a) and 350 μM iron-containing medium (b). Results are presented as a percentage of germinated seeds. Filled symbols, Wassilewskija (Ws); open symbols, *ysl1-1*; squares, seeds obtained from water-irrigated plants; triangles, seeds obtained from FeEDDHA-irrigated plants. (c) Seedlings with the Ws (a, c) or *ysl1-1* allele (b, d) germinating for 72 h on medium either lacking iron (a, b) or containing 350 μM iron (c, d).

result from the deregulation of its synthesis by the nicotianamine synthases (NAS). However, except for the *AtNAS2* gene, whose transcript was not detectable in shoots, we found no change in *AtNAS1*, *AtNAS3* or *AtNAS4* gene expression in the *ysl1* mutants (data not shown). Alternatively, AtYSL1 could transport NA alone. One consequence of its absence would thus be a reduction of NA content in *ysl1-1* seeds, which could in turn modulate the Fe content, as one of the proposed functions for NA is to scavenge free cellular Fe. However, this is very unlikely because YS transporters have been shown to discriminate between various metal chelates (DiDonato *et al.*, 2004; Koike *et al.*, 2004; Schaaf *et al.*, 2004), implying that their substrate is a metal-NA chelate rather than NA alone. Physicochemical characterization of the Fe chelates contained in mutant and wild-type seeds should give a clear-cut answer to the question of whether the decrease in Fe measured in the mutant corresponds to a decrease in Fe-NA content.

ysl1-1 seeds showed a slower rate of germination. In contrast to the Fe and NA content of the seed, this phenotype was efficiently rescued by an exogenous supply of Fe. Therefore, the germination defect is likely to result from the Fe-deficient state of the seeds rather than from a defect in Fe-NA transport during germination, which implies that seed germination does not rely on AtYSL1 activity. Two additional symptoms of Fe deficiency in *ysl1* germinating seedlings were (i) the yellow color of the cotyledons, which is consistent with the paleness of *ysl1-1* seeds (data not shown), and (ii) the lack of pink stain corresponding to anthocyanins, which may result from a loss of activity of the iron-requiring anthocyanin synthase, which requires Fe (De Carolis and De Luca, 1994). Both defects were restored when seedlings were germinated in the presence of a high amount of Fe.

AtYSL1 may also play a role in leaves, as we observed a moderate increase in the quantity of NA in leaves of *ysl1-1* mutants and as the *AtYSL1* gene is strongly expressed in the vasculature of leaves. Physiological data obtained on tomato *chloronerva* and tobacco *naat* plants demonstrate the essential role of NA in the unloading of Fe from vessels into leaves in order to provide Fe to intercostal regions (Scholz, 1989; Takahashi *et al.*, 2003). Our data on the localization of *AtYSL1* expression in the xylem parenchyma, its modulation by Fe nutrition and the accumulation of NA in *ysl1-1* mutant leaves suggest that AtYSL1 could participate in the delivery of Fe-NA from the xylem to the intercostal regions of the leaves.

The induction of *AtYSL1* expression in shoots in response to increased Fe supply suggests that AtYSL1 participates in the plant detoxification strategy. Upon treatment with an excess of Fe, *AtYSL1* expression spreads to mesophyll cells surrounding the leaf vein. As Fe(II)-NA is a rather Fenton-inactive form of Fe (von Wiren *et al.*, 1999), its transport by AtYSL1 into tissues

with detoxification capacity or into specific cellular compartments may protect the cell from oxidative damage. A role of AtYSL1 in the mechanism of response to Fe excess is further supported by the fact that *AtYSL1* and *AtFER1*, which encodes the storage protein ferritin, are quickly and coordinately induced by excess Fe treatment. Furthermore, publicly available databases indicate that *AtYSL1* expression is stronger in senescent leaves. During senescence, dismantling of chloroplasts and degradation of macromolecules lead to the release of Fe, which catalyzes the production of reactive oxygen species and produces oxidative stress. Interestingly, a ferritin gene has been shown to be upregulated in senescent leaves of *Brassica napus* (Buchanan-Wollaston and Ainsworth, 1997), where it could participate in the detoxification of cellular Fe. Similarly, AtYSL1 may protect the cell from cellular damage by Fe–NA compartmentalization or by transporting Fe–NA to specialized tissues. In pea Fe-overaccumulating mutants, the NA level was shown to parallel the Fe level and NA to accumulate in the vacuole in response to Fe overload, suggesting that NA may detoxify excess Fe through vacuolar sequestration (Pich *et al.*, 2001). It would also be interesting to determine in future experiments whether AtYSL1 in senescent leaves is expressed in intercostal regions in addition to the xylem parenchyma.

The presence of AtYSL1 in pollen and more importantly in the vasculature of the anther filament suggests that it also plays a role in the delivery of Fe to pollen grains. The role of NA in reproductive organs and more specifically in flowers has been nicely illustrated by the physiological characterization of NA-deficient tobacco *naat* plants with very abnormal and essentially sterile flowers (Takahashi *et al.*, 2003). We found that the capacity of *ysl1-1* pollen to germinate was not impaired in *in vitro* germination assays (data not shown). We also assessed the fertility of *ysl1-1* flowers by counting the number of seeds in siliques but observed no significant difference between mutant and wild type (data not shown). Further work will be needed to elucidate the physiological role of AtYSL1 in pollen.

The main finding of this work is the fact that knocking out the *AtYSL1* gene seriously affected the Fe and NA content of the seed. In contrast to tomato *chloronerva* or transgenic tobacco *naat* plants, which both show pleiotropic phenotypes and profound developmental alterations, including fertility defects, the targeted mutation of *AtYSL1* did not affect the metal content or development of the rest of the plant, allowing us to pinpoint the significant role of a YSL transporter in the loading of Fe into seeds. As Fe entry into the seeds seems to be a rate-limiting step, strategies aimed at increasing seed Fe content via overexpression of a ferritin gene are likely to be insufficient. Indeed, transgenic rice seeds accumulate relatively little Fe despite a very high production of ferritin (Qu *et al.*, 2005). In the future, one might envisage

combining these approaches with the overproduction of Fe loading systems to improve seed quality.

Experimental procedures

Plant growth

For hydroponic cultures, plants were grown under short-day conditions (8 h at $300 \mu\text{E m}^{-2} \text{sec}^{-1}$, 20°C) in a medium containing (in mM) 1.25 KNO_3 , 1.5 $\text{Ca}(\text{NO}_3)_2$, 0.75 MgSO_4 , 0.5 KH_2PO_4 and 0.1 $\text{Na}_2\text{O}_3\text{Si}$, and (in μM) 50 H_3BO_3 , 12 MnCl_2 , 0.7 CuSO_4 , 1 ZnCl_2 , 0.2 MoO_4Na_2 and 100 Fe-ethylenediaminetetraacetic acid (Fe-EDTA). The medium was changed weekly. After 5 weeks of culture, roots were washed for 3 min in a solution containing 0.3 mM bathophenanthroline-disulfonic acid (B-1375; Sigma, St. Louis, MO, USA) and 5.7 mM $\text{Na}_2\text{S}_2\text{O}_4$ (Art 6507; Merck, Darmstadt, Germany), then rinsed three times with deionized water. Plants were then grown on the medium described above without Fe-EDTA. After 5 days of Fe deprivation, 300–500 μM of Fe-EDTA was added to the medium and the plants further grown for the length of time indicated in Figures 2 and 4.

For the GUS assay on young plantlets, transgenic seeds were surface-sterilized and grown on Petri dishes in half-strength Murashige and Skoog (MS) medium (Murashige and Skoog, 1962) with 30 mM sucrose [pH adjusted to 5.2 with 2-Morpholinoethane-sulfonic acid (MES)-KOH] containing 50 mg ml^{-1} kanamycin. Plants were incubated in long-day conditions (16 h at $150 \mu\text{mol sec}^{-1} \text{m}^{-2}$, 21°C). After 10 days, resistant plantlets were transferred onto Fe-deficient (no Fe added to the media) or Fe-excess (300 μM NaFe-EDTA) plates for 5 days. Production of seeds by water- and Fe-irrigated plants: plants were cultivated on soil (Humin Substrate N2 Neuhaus; Klasmann-Deilmann, Geeste, Germany) in a greenhouse at 23°C and irrigated with water or with a solution of 600 μM FeEDDHA (0.5 g l^{-1} Sequestrene, Fertiligene, Ecully, France) for 6 weeks.

For Arabidopsis transformation, constructs were introduced into the MP90 strain of *Agrobacterium tumefaciens*, which was then used to transform Arabidopsis (ecotype Columbia) following the ‘floral dip’ method (Clough and Bent, 1998). Transformed lines expressing GUS fusions were selected on kanamycin, whereas complemented *ysl1-1* mutant lines were selected on hygromycin.

Identification of two AtYSL1 knockout alleles

The mutant lines DMR20 and SALK_034534 from the Versailles-INRA and SIGnal (Salk Institute, La Jolla, CA, USA) collections of T-DNA insertion mutants, respectively, were identified through the T-DNA insertions sequence databases. Homozygous mutated plants were isolated by PCR screening using a T-DNA left border-specific primer and an *AtYSL1* gene-specific primer (for the *ysl1-1* mutant: forward: 5'-CAGTCTCCATGGAAATAGAGC-3'; reverse: 5'-CGGGTACCAGACAACACATATGTCTTATGG-3'; for the *ysl1-2* mutant: 5'-GGCTTAATGTGGCCTCTTC-3' and LB-b1: 5'-GCGTGGACCGCTTGCTGCAACT-3'). Reverse transcriptase–polymerase chain reactions (RT-PCRs) were performed on RNA prepared from leaves of wild-type and *ysl1-1* and *ysl1-2* mutants using *AtYSL1* gene-specific primers on each side of the T-DNA insertions (*ysl1-1*: forward: 5'-CCGCTCGAGTTACGGCATCGCTGTCGG-3'; reverse: 5'-CGGGTACCAGACAACACATATGTCTTATGG-3'; *ysl1-2*: forward: 5'-GGCTTAATGTGGCCTCTTC-3'; reverse: 5'-GGACTAGTCTATGAAGCTAAGAACTTC-3') which amplify a fragment in the wild-type allele, but not in the mutant [Figure 5(b)]. *PIP2*;1 primers (forward:

5'-TGC GAAAGGATGTGGCAGCCGTTCCCGGA-3'; reverse: 5'-CAA-CGCATAAGAACCTCTTTGA-3') amplifying the aquaporin *PIP2;1* were used as a control. Segregation on kanamycin revealed a 3:1 ratio characteristic of a single T-DNA insertion in both alleles.

Plasmid constructions

***AtYSL1* cDNA cloning.** The *AtYSL1* cDNA was amplified by PCR from reverse-transcribed RNA prepared from shoots of plants grown in hydropony, as described above, and treated with 500 μ M NaFe-EDTA for 12 h. The PCR reaction was performed using thermostable DNA polymerase (pfu) polymerase (Promega, Madison, WI, USA) and the following primers: *ysl1*-ATG (5'-CAGTCTCCATGGAAATAGAGC-3'), containing a *NcoI* restriction site, and *ysl1*-STOP (5'-GGACTAGTCTTGAAGCTAAGAAGCTTC-3'), containing a *SpeI* restriction site. The *NcoI*-*SpeI*-digested *AtYSL1* cDNA was cloned into a modified pBluescript KS+ (Eyal *et al.*, 1995) previously digested with the same enzymes and completely sequenced. This vector was named pBK-YSL1.

Plasmid for GUS activity analyses. A 1.5-kb fragment of the *AtYSL1* promoter was amplified from the BAC clone T19F6 containing the *AtYSL1* gene using pfu DNA polymerase and the oligonucleotides YSL1-1 (5'-TAGGAAGCTTATATCAAAAATAAGGTGAGAC-3'), containing a *HindIII* restriction site, and YSL1-2 (5'-CTCTATTCCATGGAGACTG-3'), containing a *NcoI* restriction site. This *HindIII*-*NcoI* fragment was cloned in frame with the *uidA* gene previously inserted in pBKS+ modified as described in Eyal *et al.* (1995). The *HindIII*-*XbaI* fragment containing the *AtYSL1*-*GUS* fusion was excised from the resulting plasmid and ligated into the pBIN19 vector (Bevan, 1984) previously digested by the same enzymes. The resulting plasmid was named pBIN19-YSL1-GUS.

Plasmid for *ysl1-1* complemented lines. An *AtYSL1* gene fragment containing 1.5 kb of promoter sequence upstream of the ATG and 0.37 kb of the 3' untranslated region was amplified from the BAC clone T19F6 using the pfu polymerase and the primers YSL1-1 (see above) and 5'-CCCGAGCTCTAAAGCAAGGATTCTTCC-3', containing a *HindIII* site and a *SacI* site, respectively. The *HindIII*-*SacI* restriction fragment was subcloned into the pGreen179 binary vector digested by the same enzymes and the resulting construct was sequenced.

Metal content determination

The metal (Fe, Zn, Mn and Cu) concentrations of samples of mineralized roots and leaves were determined by atomic absorbance spectrometry. Prior to mineralization, root samples were washed as indicated in the section 'Plant growth'. All samples were ground with a mortar and pestle in liquid nitrogen. About 100 mg of dry matter was completely digested in 70% NO_3 at 120°C and solubilized in 2 ml of 70% HNO_3 and 18 ml of H_2O . The metal content was determined using a Varian SpectrAA220-FS (Varian; Palo Alto, CA, USA). In seeds, Fe content was measured as described in Lobreaux and Briat (1991), while Zn, Cu and Mn contents were measured by ICP-MS.

Nicotianamine measurement

Nicotianamine was extracted and measured as described in Neumann *et al.* (1999) with some modifications. Plant tissues were ground in liquid nitrogen and approximately 100 mg was extracted

with 300 μ l of H_2O at 80°C for 20 min and then centrifuged (18 000 *g*) for 10 min. Fifty microliters of supernatant was derivatised with an equal volume of a o-phthalaldehyde (OPA) solution (12.8 mg of OPA, 2.5 ml of methanol, 10.5 ml of 0.2 M borate buffer, pH 9.9, containing 0.1 M KCl, and 25 μ l of mercaptopyropionic acid), incubated in the dark for 1 min. One microliter of a sulfosalicylic acid solution [50%, weight/volume (w/v)] was then added, just before injection. HPLC separation was carried out on a PrepStar Solvent Delivery Module (Varian) using a binary gradient: solvent A, phosphate-citrate buffer pH 3; solvent B, methanol/tetrahydrofuran 80%/20% (v/v) gradient at a flow rate of 0.7 ml min^{-1} on a C18 Nucleodur column (250 mm \times 4.6 mm; Macherey-Nagel, Düren, Germany). Gradient parameters were 0–20 min, 0–100% B, 20–22 min, 100% B, 22–25 min, 100–0% B. Fluorescence of OPA derivatives was measured with a ProStar Fluorescence detector (Varian; excitation 350 nm; emission 455 nm), and quantification was carried out using pure chemically synthesized NA (T-Hasegawa Co., Tokyo, Japan) as external standard.

Gene expression analysis

Tri-Reagent (T9424; Sigma) was used to extract total RNA from roots and shoots of plants cultivated hydroponically as described above.

For Northern blot experiments, 15 μ g of total RNA was denatured and electrophoresed on a 1.2% 3-(*N*-morpholino)-propane-sulfonic acid/formaldehyde/agarose gel before transfer to a nylon Hybond- N^+ membrane (Amersham, Buckinghamshire, UK). The hybridizations were performed in Church buffer (Church and Gilbert, 1984). The *AtYSL1*-specific probe was generated by amplification of a 1.5-kb fragment of the cDNA including 378 bp of 3'-untranslated region (3'-UTR) sequences using the following primers : forward: 5'-ggCTTAATgTggCCTCTTC-3'; reverse: 5'-CCCgAgCTCTAAAggCAAggATTCTTCC-3'. The *AtFER1*-specific probe was obtained by fusing 281 bp of 5'-UTR located immediately upstream of the ATG with 188 bp of 3'-UTR located immediately downstream of the stop codon and was a gift from F. Gaymard (Biochimie et Physiologie, moléculaire des plantes, CNRS, Montpellier, France). The *AtEF-1 α* probe was amplified by RT-PCR on total RNA prepared from Arabidopsis suspension cells using the following gene-specific primers : forward: 5'-CCACCACTGGTGGTTTTGAGGCTGGTATC-3'; reverse: 5'-CATTGAACCAACGTTGTCACCTGGAAG-3'. Membranes were exposed to a BAS imaging plate (BAS-SR2025; Fujifilm, Tokyo, Japan) for 3, 1 and 1 days for *AtYSL1*, *AtFER1* and *AtEF-1 α* , respectively. The signal was revealed using BAS 5000 (Fujifilm).

GUS expression analysis

For enzymatic GUS assay, roots and shoots of 12 kanamycin-resistant T1 independent lines were harvested separately and ground in Eppendorf tubes in GUS extraction buffer (Jefferson *et al.*, 1987). GUS activity was measured fluorometrically using 1 mM 4-methylumbelliferyl- β -D-glucuronide as substrate (Euromedex, Mundolsheim, France). The total protein content of the samples was determined according to Bradford (1976) and used to correct for GUS activity. GUS histochemical staining was performed either on 15-day-old plantlets grown on plates or on flowers and siliques of hydroponically grown plants. 5-bromo-4-chloro-3-indolyl β -D-glucuronide was used as substrate (Euromedex). Stained leaves of plantlets grown in plates containing 50 μ M NaFe-EDTA and stained siliques harvested from soil-grown plants were embedded in hydroxyethylmethacrylate (Technovit 7100; Heraeus-Kulzer, Wehrheim, Germany) and cut into thin cross-sections (4 μ m for leaves

and 5 µm for siliques) using a Leica RM 2165 microtome (Leica, Nussloch, Germany). Cross-sections were counter-stained with Schiff dye and observed with an Olympus BH2 microscope (Olympus, Tokyo, Japan).

Acknowledgements

We thank Geneviève Conejero for assistance with histology, Laurent Querdane for performing ICP-MS analysis, and Frederic Gaymard (CNRS) for sharing *AtFER1* and *EF-1α* probes. The work of MLJ was supported by a thesis fellowship from the Ministère de l'Éducation Nationale, de la Recherche et de la Technologie, and the work of AS was supported by an INRA postdoctoral fellowship. This work was funded by Centre National de la Recherche Scientifique and INRA and by the Toxicologie Nucléaire program of the Réseau Inter-Organismes (RIO).

References

- Bevan, M.** (1984) Binary Agrobacterium vectors for plant transformation. *Nucl. Acids Res.* **12**, 8711–8721.
- Bradford, M.M.** (1976) A rapid and sensitive method for the quantitation of microgram quantities of protein utilizing the principle of protein-dye binding. *Anal. Biochem.* **72**, 248–254.
- Buchanan-Wollaston, V. and Ainsworth, C.** (1997) Leaf senescence in *Brassica napus*: cloning of senescence related genes by subtractive hybridisation. *Plant Mol. Biol.* **33**, 821–834.
- Church, G.M. and Gilbert, W.** (1984) Genomic sequencing. *Proc. Natl Acad. Sci. USA*, **81**, 1991–1995.
- Clough, S.J. and Bent, A.F.** (1998) Floral dip: a simplified method for Agrobacterium-mediated transformation of *Arabidopsis thaliana*. *Plant J.* **16**, 735–743.
- Connolly, E.L., Fett, J.P. and Gueriot, M.L.** (2002) Expression of the IRT1 metal transporter is controlled by metals at the levels of transcript and protein accumulation. *Plant Cell*, **14**, 1347–1357.
- Connolly, E.L., Campbell, N.H., Grotz, N., Prichard, C.L. and Gueriot, M.L.** (2003) Overexpression of the FRO2 ferric chelate reductase confers tolerance to growth on low iron and uncovers posttranscriptional control. *Plant Physiol.* **133**, 1102–1110.
- Curie, C. and Briat, J.F.** (2003) Iron transport and signaling in plants. *Annu. Rev. Plant Biol.* **54**, 183–206.
- Curie, C., Panaviene, Z., Loulergue, C., Dellaporta, S.L., Briat, J.F. and Walker, E.L.** (2001) Maize yellow stripe1 encodes a membrane protein directly involved in Fe(III) uptake. *Nature*, **409**, 346–349.
- De Carolis, E. and De Luca, V.** (1994) 2-oxoglutarate-dependent dioxygenase and related enzymes: biochemical characterization. *Phytochemistry*, **36**, 1093–1107.
- DiDonato, R.J., Jr, Roberts, L.A., Sanderson, T., Eisley, R.B. and Walker, E.L.** (2004) Arabidopsis yellow stripe-like2 (YSL2) : a metal-regulated gene encoding a plasma membrane transporter of nicotianamine-metal complexes. *Plant J.* **39**, 403–414.
- Eide, D., Broderius, M., Fett, J. and Gueriot, M.L.** (1996) A novel iron-regulated metal transporter from plants identified by functional expression in yeast. *Proc. Natl Acad. Sci. USA*, **93**, 5624–5628.
- Eyal, Y., Curie, C. and McCormick, S.** (1995) Pollen specificity elements reside in 30 bp of the proximal promoters of two pollen-expressed genes. *Plant Cell*, **7**, 373–384.
- Grusak, M.A.** (1994) Iron transport to developing ovules of *Pisum sativum*. I. Seed import characteristics and phloem iron-loading capacity of source regions. *Plant Physiol.* **104**, 649–655.
- Henriques, R., Jasik, J., Klein, M., Martinoia, E., Feller, U., Schell, J., Pais, M.S. and Koncz, C.** (2002) Knock-out of Arabidopsis metal transporter gene IRT1 results in iron deficiency accompanied by cell differentiation defects. *Plant Mol. Biol.* **50**, 587–597.
- Higuchi, K., Nishizawa, N.K., Römheld, V., Marschner, H. and Mori, S.** (1996) Absence of nicotianamine synthase activity in the tomato mutant *chloronerva*. *J. Plant Nutr.* **19**, 123–129.
- Jefferson, R.A., Kavanagh, T.A. and Bevan, M.W.** (1987) GUS fusions: beta-glucuronidase as a sensitive and versatile gene fusion marker in higher plants. *EMBO J.* **6**, 3901–3907.
- Koh, S., Wiles, A.M., Sharp, J.S., Naider, F.R., Becker, J.M. and Stacey, G.** (2002) An oligopeptide transporter gene family in Arabidopsis. *Plant Physiol.* **128**, 21–29.
- Koike, S., Inoue, H., Mizuno, D., Takahashi, M., Nakanishi, H., Mori, S. and Nishizawa, N.K.** (2004) OsYSL2 is a rice metal-nicotianamine transporter that is regulated by iron and expressed in the phloem. *Plant J.* **39**, 415–424.
- Krüger, C., Berkowitz, O., Stephan, U.W. and Hell, R.** (2002) A metal-binding member of the late embryogenesis abundant protein family transports iron in the phloem of *Ricinus communis* L. *J. Biol. Chem.* **30**, 30.
- Ling, H.Q., Koch, G., Baumlein, H. and Ganai, M.W.** (1999) Map-based cloning of chloronerva, a gene involved in iron uptake of higher plants encoding nicotianamine synthase. *Proc. Natl Acad. Sci. USA*, **96**, 7098–7103.
- Lobreaux, S. and Briat, J.F.** (1991) Ferritin accumulation and degradation in different organs of pea (*Pisum sativum*) during development. *Biochem. J.* **274**, 601–606.
- Lobreaux, S., Massenet, O. and Briat, J.F.** (1992) Iron induces ferritin synthesis in maize plantlets. *Plant Mol. Biol.* **19**, 563–575.
- Murashige, T. and Skoog, F.** (1962) A revised medium for rapid growth and bioassays with tobacco tissue cultures. *Physiol. Plant.* **15**, 473–497.
- Neumann, G., Haake, C. and Römheld, V.** (1999) An improved HPLC method for determination of phytosiderophores in root washings and tissue extracts. *Plant Nutr.* **22**, 1389–1402.
- Nguyen, H., Brown, R. and Lemmon, B.** (2000) The specialized chalazal endosperm in *Arabidopsis thaliana* and *Lepidium virginicum* (Brassicaceae). *Protoplasma*, **212**, 99–110.
- Otegui, M.S., Capp, R. and Staehelin, L.A.** (2002) Developing seeds of Arabidopsis store different minerals in two types of vacuoles and in the endoplasmic reticulum. *Plant Cell*, **14**, 1311–1327.
- Pich, A., Manteuffel, R., Hillmer, S., Scholz, G. and Schmidt, W.** (2001) Fe homeostasis in plant cells: does nicotianamine play multiple roles in the regulation of cytoplasmic Fe concentration? *Planta*, **213**, 967–976.
- Qu, L.Q., Yoshihara, T., Ooyama, A., Goto, F. and Takaiwa, F.** (2005) Iron accumulation does not parallel the high expression level of ferritin in transgenic rice seeds. *Planta*, **222**, 225–233.
- Roberts, L.A., Pierson, A.J., Panaviene, Z. and Walker, E.L.** (2004) Yellow stripe1. Expanded roles for the maize iron-phytosiderophore transporter. *Plant Physiol.* **135**, 112–120.
- Robinson, N.J., Procter, C.M., Connolly, E.L. and Gueriot, M.L.** (1999) A ferric-chelate reductase for iron uptake from soils. *Nature*, **397**, 694–697.
- Römheld, V. and Marschner, H.** (1986) Mobilization of iron in the rhizosphere of different plant species. *Adv. Plant Nutr.*, **2**, 155–204.
- Schaaf, G., Ludewig, U., Erenoglu, B.E., Mori, S., Kitahara, T. and von Wirén, N.** (2004) ZmYS1 functions as a proton-coupled symporter for phytosiderophore- and nicotianamine-chelated metals. *J. Biol. Chem.* **279**, 9091–9096.
- Schaaf, G., Schikora, A., Häberle, J., Vert, G.A., Ludewig, U., Briat, J.F., Curie, C. and von Wirén, N.** (2005) A putative function of the Arabidopsis Fe-Phytosiderophore transporter homolog AtYSL2 in Fe and Zn homeostasis. *Plant Cell Physiol.* **46**, 762–774.
- Scholz, G.** (1989) Effect of nicotianamine on iron re-mobilization in de-rooted tomato seedlings. *Biol. Met.*, **2**, 89–91.

- Stephan, U.W., Schmidke, I., Stephan, V.W. and Scholz, G.** (1996) The nicotianamine molecule is made-to-measure for complexation of metal micronutrients in plants. *Biometals*, **9**, 84–90.
- Takagi, S.I., Nomoto, K. and Takemoto, T.** (1984) Physiological aspect of mugineic acid, a possible phytosiderophore of graminaceous plants. *J. Plant Nutr.* **7**, 1–5.
- Takahashi, M., Terada, Y., Nakai, I., Nakanishi, H., Yoshimura, E., Mori, S. and Nishizawa, N.K.** (2003) Role of nicotianamine in the intracellular delivery of metals and plant reproductive development. *Plant Cell*, **15**, 1263–1280.
- Varotto, C., Maiwald, D., Pesaresi, P., Jahns, P., Salamini, F. and Leister, D.** (2002) The metal ion transporter IRT1 is necessary for iron homeostasis and efficient photosynthesis in *Arabidopsis thaliana*. *Plant J.* **31**, 589–599.
- Vert, G., Grotz, N., Dedaldechamp, F., Gaymard, F., Guerinot, M.L., Briat, J.F. and Curie, C.** (2002) IRT1, an arabidopsis transporter essential for iron uptake from the soil and for plant growth. *Plant Cell*, **14**, 1223–1233.
- Vert, G.A., Briat, J.F. and Curie, C.** (2003) Dual regulation of the Arabidopsis high-affinity root iron uptake system by local and long-distance signals. *Plant Physiol.* **132**, 796–804.
- von Wiren, N., Mori, S., Marschner, H. and Romheld, V.** (1994) Iron inefficiency in maize mutant *ys1* (*Zea mays* L. cv yellow-stripe) is caused by a defect in uptake of iron phytosiderophores. *Plant Physiol.* **106**, 71–77.
- von Wiren, N., Klair, S., Bansal, S., Briat, J.F., Khodr, H., Shioiri, T., Leigh, R.A. and Hider, R.C.** (1999) Nicotianamine chelates both FeIII and FeII. Implications for metal transport in plants. *Plant Physiol.* **119**, 1107–1114.
- Yen, M.R., Tseng, Y.H. and Saier, M.H.** (2001) Maize yellow stripe1, an iron-phytosiderophore uptake transporter, is a member of the oligopeptide transporter (OPT) family. *Microbiology*, **147**, 2881–2883.